Available online at www.sciencedirect.com
ScienceDirect
Solid State Communications 146 (2008) 25–29
solid state communications
www.elsevier.com/locate/ssc

Influence of iron ions on the magnetic properties of $CaO–SiO_2–P_2O_5–Na_2O–Fe_2O_3$ glass–ceramics

Rajendra Kumar Singh[a], G.P. Kothiyal[b], A. Srinivasan[a,*]

[a] *Department of Physics, Indian Institute of Technology Guwahati, Guwahati-781039, India*
[b] *Glass and Glass Ceramic Technology Section, TP&PED, B.A.R.C., Mumbai-400085, India*

Received 1 November 2007; received in revised form 20 January 2008; accepted 21 January 2008 by P. Chaddah
Available online 31 January 2008

Abstract

Room temperature Electron Paramagnetic Resonance (EPR) spectra and temperature dependent magnetic susceptibility measurements have been performed on $41CaO.(52-x)SiO_2.4P_2O_5.xFe_2O_3.3Na_2O$ ($2 \leq x \leq 10$ mol%) glass–ceramics. The parent glass samples were prepared by quenching the homogenized melt from 1550 °C. The glasses were then heat-treated at 1050 °C for 3 h and slowly cooled to room temperature to yield glass–ceramics. EPR and high temperature magnetic susceptibility measurements were made to elucidate the state of Fe^{+3} ions in the glass–ceramics. The EPR absorption line centered at $g \approx 4.3$ disappeared at higher concentrations of Fe_2O_3. The intensity and linewidth of the absorption line centered at $g \approx 2.1$ increased as the Fe_2O_3 concentration was increased. Information about the structural changes involving iron ions, their valence state and type of magnetic interactions between the Fe ions was obtained using EPR and magnetic susceptibility measurements. The temperature dependence of the magnetization of the glass–ceramics with low Fe_2O_3 concentrations exhibit both ferrimagnetic and paramagnetic contributions. The results obtained have been used to understand the structural changes occurring in the vicinity of iron ions and the nature of magnetic interactions between the iron ions in these glass–ceramics.

PACS: 75.30.Cr; 75.30.Et; 75.60.Ej; 75.50.Gg

Keywords: A. Magnetic material; D. Superexchange; E. Electron spin resonance; E. Magnetometry

1. Introduction

Glass–ceramics containing a magnetic phase in a biocompatible glassy matrix could be used as thermoseeds for hyperthermia treatment of cancer [1–3]. When such a magnetic glass–ceramic (MGC) piece implanted close to cancerous tissue is exposed to an alternating magnetic field, the heat generated by magnetic hysteresis loss kills the infected tissue. Attempts are being made to develop $CaO–SiO_2–P_2O_5–Na_2O$ based MGC systems with FeO and/or Fe_2O_3 [4–8]. However, no detailed investigations on the evolution of magnetic properties and biocompatibility of these MGC have been reported so far. The MGCs has magnetite as a major crystalline phase along with apatite and wollastanite, which are bone minerals. The valence state and behavior of iron in glass–ceramic provide information about the structure of the glass–ceramic and help in interpreting its magnetic properties. Electron paramagnetic resonance (EPR) studies of glass–ceramics containing transition metal ions have been used to obtain information regarding the glass–ceramic network and to identify the site symmetry around the transition metal ions. Iron ions exist in different valence states with different local symmetry in the glass matrices, for example, as Fe^{+3} with both tetrahedral and octahedral coordination, and/or as Fe^{+2} with octahedral coordination. Though Fe^{+3} and Fe^{+2} ions are both paramagnetic, only Fe^{+3} ($3d^5$, $^6S_{5/2}$) shows EPR absorptions at room temperature [9,10]. EPR spectra of Fe^{+3} ions in oxide glasses and glass–ceramics are generally characterized by the appearance of resonance absorptions at $g \approx 4.3$ and 2.1 with their relative intensity being strongly dependent on composition [11–16].

* Corresponding author. Tel.: +91 361 258 2011; fax: +91 361 258 2014.
E-mail addresses: k.rajendra@iitg.ernet.in (R.K. Singh), gpkoth@barc.gov.in (G.P. Kothiyal), asrini@iitg.ernet.in (A. Srinivasan).

0038-1098/$ - see front matter © 2008 Elsevier Ltd. All rights reserved.
doi:10.1016/j.ssc.2008.01.023

The $g \approx 4.3$ resonance line is characteristic of isolated Fe^{+3} ions predominantly situated in rhombically distorted octahedral or tetrahedral oxygen environments. The $g \approx 2.1$ resonances are assigned to those ions which interact by a superexchange coupling and can be considered as distributed in clusters [11–16]. Magnetic susceptibility measurements reveal the nature of interaction between the iron ions apart from providing information on the valence states of iron ions. In this paper, the structural changes and magnetic interactions of iron ions in $CaO–SiO_2–P_2O_5–Na_2O–Fe_2O_3$ glass–ceramics samples are investigated using EPR and magnetic susceptibility data.

2. Experimental

High purity SiO_2, Fe_2O_3, Na_2CO_3, $CaCO_3$ and $NH_4(H_2PO_4)$ were used to prepare glasses with compositions $41CaO(52-x)SiO_2 4P_2O_5 x Fe_2O_3 3Na_2O$ ($2 \le x \le 10$ mol% Fe_2O_3). The charge corresponding to the nominal compositions were melted in a platinum crucible at 1550 °C after providing for proper calcinations at 800 °C. The melt was then poured into a preheated graphite mould to form glass. The as-quenched glasses were then heat-treated at 1050 °C for 3 h and slowly cooled to room temperature to form glass–ceramics. A powder X-ray diffractometer (Seifert 3003 T/T) was used to confirm the amorphous nature of the as-quenched glasses and to identify the crystalline phases in the corresponding glass–ceramics. The data bank from the International Center for Diffraction Data (ICDD) was used for phase identification. EPR measurements were performed on a JEOL Spectrometer (model JES-FA200) operating at X-band frequency ($\nu = 9.4$ GHz) with 100 kHz magnetic field modulation at room temperature using samples in powder form. Reference signals of Mn^{2+} ions in MgO were used for standardization of linewidth and effective g-value. Magnetic susceptibility of solid glass–ceramic samples was obtained from temperature dependent magnetization measurements carried out over a temperature range of 30 °C to 780 °C at a constant applied field of 79.6 kA/m using a Vibrating Sample Magnetometer (VSM, Lakeshore 7410) equipped with a high temperature oven. The VSM was calibrated using a standard reference (high purity nickel sphere), supplied with the instrument.

3. Results and discussion

3.1. ESR studies

X-ray diffraction (XRD) patterns of the glass–ceramic samples confirmed the presence of hydroxyapatite [$Ca_{10}(PO_4)_6(OH)_2$], wollastonite [$CaSiO_3$] and magnetite [Fe_3O_4] as major crystalline phases [17]. The average crystallite size of the magnetite phase increased in the samples as the iron oxide concentration was increased from 2 to 10 mol% as depicted in Fig. 1. The EPR spectra of $41CaO(52-x)SiO_2 4P_2O_5 x Fe_2O_3 3Na_2O$ ($2 \le x \le 10$ mol%) glass–ceramic samples are shown in Fig. 2. The spectra mainly consist of absorption lines centered at $g \approx 4.3$ and $g \approx 2.0$ which are due to Fe^{+3} ions ($3d5^6S_{5/2}$). The

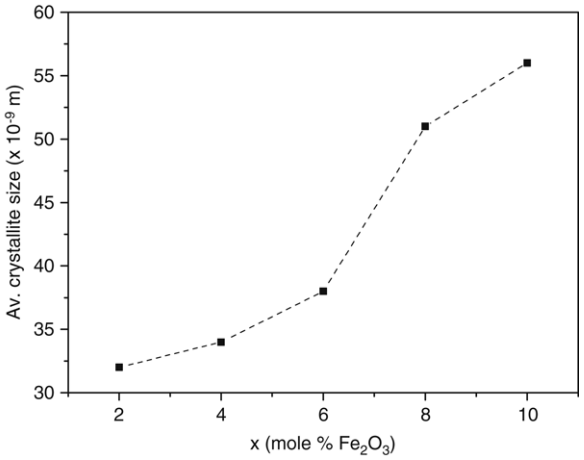

Fig. 1. Variation of average magnetite crystallite size as a function of iron oxide concentration.

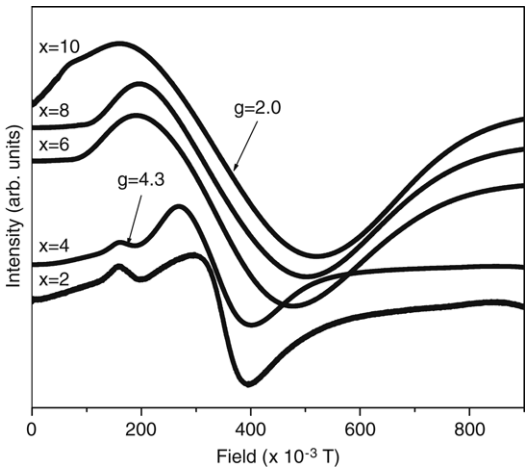

Fig. 2. Room temperature ESR absorption spectra of $41CaO.(52-x)SiO_2.4P_2O_5.xFe_2O_3.3Na_2O$ glass–ceramic samples.

relative intensity and linewidth of these absorption lines show a strong dependence on Fe_2O_3 concentration. In general the spin Hamiltonian can be expressed as [18]

$$H = \beta g \cdot H \cdot S + D\left[S_z^2 - \frac{1}{3}S(S+1)\right] + E(S_x^2 - S_y^2) \qquad (1)$$

where S_x, S_y, S_z, are components of spin along three mutually perpendicular crystalline axes x, y, and z, D and E are the usual second-order crystal field terms with axial and rhombic symmetry, and H is the applied field, respectively. If D and E are zero, the g value is expected to lie very near the free electron value of 2.0. If D or E is large as compared with $g\beta H$, in the two limiting cases of $D \neq 0$, $E = 0$, and $D = 0$, $E \neq 0$, the energy levels in zero magnetic field are easily found to be three Kramers doublets. In the first case ($D \neq 0$, $E = 0$), the lowest doublet has the effective g value $g \approx 2.0$ and $g \approx 6.0$. In the second case ($E \neq 0$, $D = 0$), the middle doublet has an isotropic g value of 4.3. Castner et al. [19] were the first to apply the spin Hamiltonian given in Eq. (1) to the $g \approx 4.3$ absorption line of Fe^{+3} ions in glass and Wickman et al. [20] identified the origin of the $g \approx 4.3$ resonance as Fe^{+3} ions in sites which

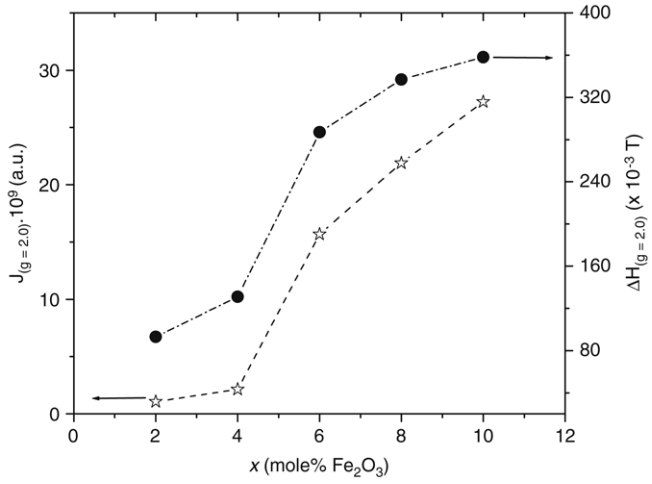

Fig. 3. Composition dependence of intensity and linewidth for $g \approx 2.1$ absorption line of $41CaO.(52-x)SiO_2.4P_2O_5.xFe_2O_3.3Na_2O$ glass–ceramic samples.

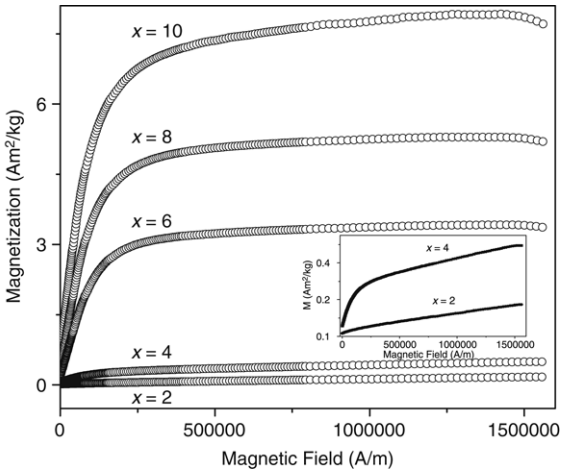

Fig. 4. Variation of room temperature magnetisation as a function of applied magnetic field for $41CaO.(52-x)SiO_2.4P_2O_5.xFe_2O_3.3Na_2O$ glass–ceramic samples. Inset shows M–H plots for the samples with $x = 2$ and 4 mol% Fe_2O_3.

have undergone rhombic distortion from cubic symmetry. The generalized spin Hamiltonian has been diagonalised within the $S = 5/2$ manifold, with $0 < \lambda(=E/D) < 1/3$ exhausting the physically acceptable possibilities. In particular, the resonance at $g \approx 2.0$ and 6.0 are the parallel and perpendicular g values of Kramers doublets when $\lambda = E/D = 0$. The isotropic resonance at $g \approx 4.3$ corresponds to $\lambda = E/D = 1/3$. This assignment identifies the feature at $g \approx 2.0$ with weak crystal field terms and the feature at $g \approx 4.3$ with the rhombic distortions of the crystal field about a site of tetrahedral or octahedral symmetry.

The concentration dependence of the EPR parameters of the MGC samples is plotted in Fig. 3 for the absorption line centered at $g \approx 2.0$. The variations in the EPR parameters, viz., the relative peak to peak height I, the linewidth of the derivative plots ΔH, and the intensity of the absorption line J, approximated as $J = I(\Delta H)^2$ of the absorption at $g \approx 2.0$ are plotted in Fig. 3. It is apparent from Fig. 3 that the intensity ($J_{(g=2.0)}$) and linewidth ($\Delta H_{(g=2.0)}$) of the $g \approx 2.0$ absorption line increase as function of x. The $g \approx 2.0$ resonance arises due to the formation of iron clusters which give rise to superexchange type interaction between iron ions. The increase in $J_{(g=2.0)}$ as a function of iron oxide content indicates an increase in the ferrimagnetically coupled superexchange type interactions in the glass–ceramic samples. However, the nonlinear increase of $J_{(g=2.0)}$ and $\Delta H_{(g=2.0)}$ with Fe_2O_3 concentration depicted in Fig. 3 shows that iron irons are present as Fe^{3+} as well as Fe^{2+} in the samples. Fe^{2+} ions are not involved in the EPR absorption but their interactions with Fe^{3+} influence the characteristics of the absorption lines. Superexchange mechanisms tend to narrow the absorption line. On the other hand, interactions between Fe^{3+} and Fe^{2+} ions tend to broaden the linewidth. The final linewidth depends on the relative strengths of the two mechanisms influencing the linewidth. The increase in the linewidth of the $g \approx 2.0$ resonance with Fe_2O_3 concentration signifies the dominance of the broadening mechanisms as the Fe_2O_3 content is increased, which in turns indicates an increase in Fe^{2+} ion concentration as a function of Fe_2O_3 concentration in the glass–ceramic samples. It can be observed in Fig. 2 that the $g \approx 2.0$ line shifts from 0.342 T (or $g = 1.971$) for the $x = 2$ mol% sample to 0.326 T (or $g = 2.069$) for the $x = 10$ mol% sample. This shift can be attributed to an increase in ferrimagnetic multi-domain crystallites in the samples. It is worthy to point out that the average magnetite crystallite size increases in the samples as a function of x.

Fig. 2 shows that the EPR absorption line at $g \approx 4.3$ is observed only in samples with $x = 2$ and 4 mol% Fe_2O_3. The intensity ($J_{(g=4.3)}$) and linewidth ($\Delta H_{(g=4.3)}$) of the $g \approx 4.3$ absorption line decreases as x is increased. Since the $g \approx 4.3$ line arises from Fe^{+3} ions in low symmetry sites, the disappearance of the $g \approx 4.3$ line signifies a decrease of low symmetry sites at Fe^{+3} ions and a corresponding increase in Fe^{+3} sites of higher symmetry in the crystallization process. In other words, the EPR spectra indicate that low symmetry sites whose crystal fields are equal and very near to the special crystal fields with $D = 0$, $E \neq 0$ and $\lambda = E/D = 1/3$ have been removed during the crystallization process. As already pointed out, XRD studies have confirmed that magnetite ($Fd\bar{3}m$) crystallizes when the glasses are heat-treated.

3.2. Magnetisation and susceptibility

Fig. 4 shows the initial magnetization curves for all samples measured at room temperature. The magnetization curves of the $x = 2$ and 4 samples are not saturated up to an applied magnetic field of 1592 kA/m as can bee seen from the inset of Fig. 4. It can be inferred from the nature of the curves that the samples with $x = 2$ and 4 mol% Fe_2O_3 exhibit a combination of paramagnetic and ferrimagnetic behaviour. Such behaviour has also been reported in annealed CaO–P_2O_5–Fe_2O_3 glasses [21]. A comparison with the EPR spectra of these samples shown in Fig. 2 would clarify that both these techniques yield results that support and complement each other. The magnetization curves of samples with $x = 6$, 8, and 10 are saturated at

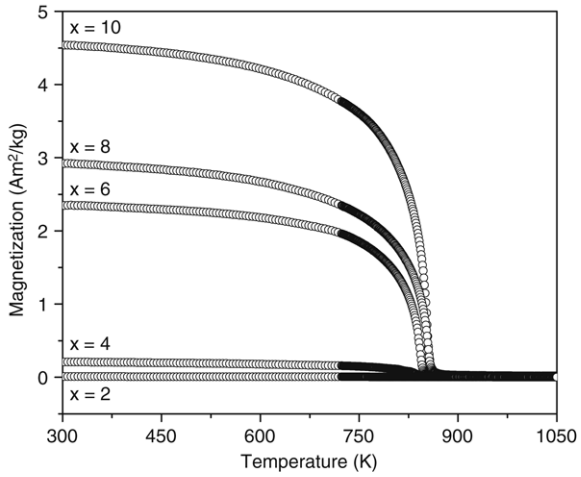

Fig. 5. Variation of magnetization as a function of temperature of $41CaO.(52-x)SiO_2.4P_2O_5.xFe_2O_3.3Na_2O$ glass–ceramics samples.

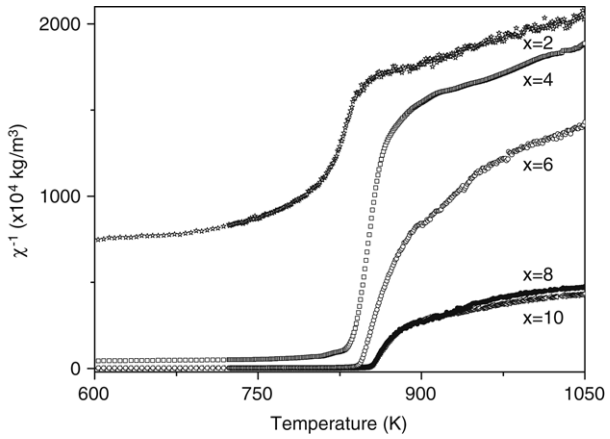

Fig. 6. Plots of temperature dependent reciprocal magnetic susceptibility of $41CaO.(52-x)SiO_2.4P_2O_5.xFe_2O_3.3Na_2O$ ($x = 2, 4, 6, 8, 10$ mol% iron oxide) glass–ceramic samples.

magnetic field 1592 kA/m. These compositions exhibit only ferrimagnetic behavior. It is interesting to note that the EPR spectra of these compositions show only one absorption line at $g \approx 2.1$, which is an indication of enhanced magnetic superexchange interaction between the iron ions.

Fig. 5 shows that plots of magnetization as a function of temperature (M–T curve) under a constant magnetic field of 79.6 kA/m for all the MBC samples. During heating, a steady decrease in magnetization is observed. The ferrimagnetic behavior of the investigated samples is obvious from the nature of the M–T curves. The variation of inverse magnetic susceptibility (χ^{-1}) with temperature over the range of 600 to 1050 K is shown in Fig. 6. The χ^{-1}–T plots which are nearly linear above 950 K show a downward drop at low temperatures. The deviation from linearity and the systematic downward drop of χ^{-1}–T curves indicate the onset of short-range order just above the ferrimagnetic Neel temperature (T_N). The heat treatment given to the glass samples modifies the internal network structure of the specimen and induces increased crystallization of magnetite in samples with higher x due to an increase in Fe^{3+} ions. Comparison with the literature [22] reveals that the main contribution to magnetization in these glass–ceramics comes from iron ions in magnetite (Fe_3O_4). The Neel temperature (T_N) of the glass–ceramic samples increases from 830 to 853 K as x is varied from 2 to 10 mol%. The Néel temperature increase with increase in Fe_2O_3 concentration may be correlated with the corresponding increase in the intensity of the $g \approx 2.0$ resonance line (Fig. 3). A closer look at Fig. 6 would show a departure in the manner in which inverse susceptibility decreases as temperature is lowered in the case of the $x = 2$ and $x = 4$ samples *vis-a-vis* the $x \geq 6$ samples. χ^{-1} should tend to zero at $T = T_N$ if the sample is entirely ferrimagnetic. Any departure from this behaviour as observed in the case of samples with $x = 2$ and 4 shows the coexistence of a paramagnetic phase along with the ferrimagnetic phase in these samples.

4. Conclusions

EPR absorptions due to Fe^{3+} were detected in the glass–ceramic system $41CaO.(52-x)SiO_2.4P_2O_5.xFe_2O_3.3Na_2O$ ($2 \leq x \leq 10$ mol%). The structure of the EPR spectra and the EPR parameters strongly depend of the iron ion concentrations. At higher concentrations of Fe_2O_3, the disappearance of the $g \approx 4.3$ absorption line signifies that Fe^{3+} sites occupy higher symmetry sites. Broadening of the $g \approx 2.0$ absorption linewidth as a function x indicates the presence of Fe^{2+} ions along with Fe^{3+} ions in the glass–ceramics. The shift in the $g \approx 2.0$ resonance towards lower g values as a function of x signifies the formation of ferrimagnetic multi-domain crystallites. The combined EPR and magnetic property studies provide useful insight on the nature and role of iron ions in this MBC system.

Acknowledgements

Financial assistance from Board of Research in Nuclear Sciences, Department of Atomic Energy, India, through a collaborative research project No. 2005/34/15/BRNS and Department of Science and Technology, India *vide* project No: SR/S2/CMP-19/2006 are gratefully acknowledged.

References

[1] K. Ohura, M. Ikenaga, T. Nakamura, T. Yamamuro, Y. Ebisawa, T. Kokubo, Y. Kotoura, M. Oka, J. Appl. Biomat. 2 (1991) 153.
[2] M. Kawashita, S. Domi, Y. Saito, M. Aoki, Y. Ebisawa, T. Kokubo, T. Saito, M. Takano, N. Araki, M. Hiraoka, J. Mater. Sci. Mater. Med. (2008), doi:10.1007/s10856-007-3262-8.
[3] Y.K. Lee, S.B. Lee, Y.-U. Kim, K.N. Kim, S.-Y. Choi, K.H. Lee, I.B. Shim, C.-S. Kim, J. Mater. Sci. 38 (2003) 4221.
[4] O. Bretcanu, S. Spriano, C.B. Vitale, E. Verne, J. Mater. Sci. 41 (2006) 1029.
[5] T. Leventouri, A.C. Kis, J.R. Thompson, I.M. Anderson, Biomater. 26 (2005) 4924.
[6] Y. Ebisawa, F. Miyaji, T. Kokubo, K. Ohura, T. Nakamura, Biomater. 18 (1997) 1277.
[7] O. Bretcanu, E. Verne, M. Coisson, P. Tiberto, P. Allia, J. Magn. Magn. Mater. 305 (2006) 529.
[8] O. Bretcanu, S. Spriano, E. Verne, M. Coisson, P. Tiberto, P. Allia, Acta Biomater. 1 (2005) 421.
[9] M. Lacovacci, E.C. da Silva, H. Vargas, E.A. Pinheiro, F. Galembeck,

L.C.M. Miranda, J. Appl. Phys. 65 (1989) 5150.
[10] M.L. Baesso, E.C. Siliva, F.C.G. Gandro, H. Vargas, Phys. Chem. Glasses 31 (1990) 122.
[11] D. Eniu, D. Cacaina, M. Coldea, M. Valeanu, S. Simon, J. Magn. Magn. Mater 293 (2005) 310.
[12] T. Komastu, N. Soga, J. Chem. Phys. 72 (1980) 1781.
[13] K. Tanaka, N. Soga, R. Ota, K. Hirao, Bull. Chem. Soc. Jpn. 59 (1986) 1079.
[14] A.K. Bandyopadhyay, J. Zarzycki, P. Auric, J. Chappert, J. Non-Cryst. Solids 40 (1980) 353.
[15] S. Simon, D. Eniu, A. Pasca, D. Dadarlat, V. Simon, Mod. Phys. Lett. B15 (2001) 921.
[16] T. Komatsu, N. Soga, J. Mater. Sci. 19 (1984) 2353.
[17] R.K. Singh, G.P. Kothiyal, A. Srinivasan, J. Magn. Magn. Mater. (2008), doi:10.1016/j.jmmm.2007.11.007.
[18] B. Bleaney, K.W.H. Stevens, Rep. Prog. Phys. 16 (1953) 108.
[19] T. Castner Jr., G.S. Newell, W.C. Holton, C.P. Slichter, J. Chem. Phys. 32 (1960) 668.
[20] H.H. Wickman, M.P. Klein, D.A. Shirley, J. Chem. phys. 42 (1965) 2113.
[21] B. Kumar, C.H. Chen, J. Appl. Phys. 75 (1994) 6760.
[22] J.A. Kerr, in: D.R. Lide (Ed.), CRC Handbook of Chem. Phys., 81st ed., CRC Press, Boca Raton USA, 2000.